ELSEVIER

Polymer 43 (2002) 1429–1436

polymer

www.elsevier.com/locate/polymer

Surface phase morphology and composition of the casting films of PVDF–PVP blend

Ningping Chen, Liang Hong*

Department of Chemical and Environmental Engineering, National University of Singapore, 10 Kent Ridge Crescent, Singapore, 119260

Received 23 February 2001; received in revised form 1 August 2001; accepted 24 September 2001

Abstract

Films of a binary polymer blend comprising of hydrophobic poly(vinylidene fluoride) (PVDF) and hydrophilic poly(vinylpyrrolidone) (PVP) have been prepared by solution-casting. The dependence of surface structure and composition of the films on the PVP content in the blend was investigated by using atomic force microscope (AFM), XRD, XPS, SEM and differential scanning calorimeter (DSC). It has been found that the interaction between the two homopolymers prevents PVDF from crystallization in the blend, the net result of which has a primary effect on the surface properties of the films. PVP has a greater concentration at the surface than in the bulk as long as PVDF crystallizes in the bulk during the film formation process, which leaves a thermodynamically non-equilibrium surface state. On the other hand, with an increase in the PVP content, the interaction between segmental PVDF and PVP in the beginning transforms the crystalline state of PVDF from α to γ phase, and finally results in the disappearance of crystalline PVDF phases. A meager crystallization of PVDF segments could still carry on at the surface of a film with a miscible (or an amorphous) bulk; this occurrence makes the surface more hydrophobic than its bulk phase.

Keywords: Surface enrichment; Amphiphilic polymer blend; Surface morphology

1. Introduction

In a multicomponent polymer blend, the surface enrichment phenomenon would occur provided there is a difference in the surface free energy of each component [1–6], which reflects the spontaneity that a component with lower free energy in the blend would take up more surface positions in order to minimize the interfacial free energy at the air–polymer interface. The effect of the miscibility between components on surface composition has been studied by several groups with using binary blends, such as poly(styrene)/deuterated-poly(styrene), PS/poly(vinylmethylether) and poly(methylmathacrylate)/poly(vinylchloride) [7–10]. Their studies showed that the surface of the blends was enriched by the lower surface energy component regardless of compatibility in the blends. In other words, the low surface energy component has a higher concentration at the surface than in the bulk. Moreover, there are some exceptional cases, such as the poly(styrene)/poly(ethylene oxide) (PS/PEO) system. As PS clearly has a much lower surface free energy than PEO, it is expected that PS should be enriched at surface of the blend. However, in reality, the surface is not engulfed in PS despite the fact that the system was subjected to annealing at 130°C [11]. This divergence suggests that some other variables also take part in shaping the final surface structure and composition. In this particular case, the crystallization propensity of PEO is believed to reverse the surface enrichment sequence.

As poly(vinylidene fluoride) (PVDF) is known to possess a low free energy at the interface with air ($\gamma = 26.0$ mN m^{-1}), it is an appropriate material for conducting studies of the surface enrichment effect. And more importantly, PVDF is compatible with several types of oxygen-containing polymers such as the acrylate polymers [12–16]. In principle, the miscibility can be attributed to the existence of a quasi-hydrogen bonding between these two sorts of polymers. This unique property, in addition to its good mechanical strength and environmental resistance, renders PVDF an ideal candidate for blending with an oxygen-containing hydrophilic polymer for applications that need both hydrophilicity and mechanical strength. In this paper, the emphasis will be placed on the surface structure of the binary blend consisting of PVDF and poly(vinylpyrrolinidone) (PVP) instead of the compatibility between the two polymers; the latter has been reported [17,18].

* Corresponding author.
E-mail address: chehongl@nus.edu.sg (L. Hong).

0032-3861/02/$ - see front matter
PII: S0032-3861(01)00671-1

2. Experimental

2.1. Materials and film preparations

PVDF (Mw = 534,000, Aldrich) and PVP (Mw = 360,000, ISP Technologies Inc) were used as received. PVDF and PVP were dissolved in dimethylformamide (DMF, Merk) and the resulting solution was spread on a glass substrate. A freestanding sheet of the polymer blend (with a thickness of about 100 μm) was then obtained after drying under vacuum at 80°C for 48 h. Some samples were annealed at 120°C for 48 h by a gradual heating rate under nitrogen atmosphere. In the following sections, the abbreviation DFVP*ij* will be used to denote the casting films of this binary blend with different compositions, where *i* and *j* are the portions by weight of PVDF and PVP, respectively.

2.2. Instrumental analysis

Thermal analysis was performed on a NETZSCH differential scanning calorimeter (DSC) 200 differential scanning calorimeter (DSC) and the temperature range of scanning was from −20 to 200°C at a heating rate of 10°C/min. The crystalline structure of PVDF was determined on an X-ray diffractometer (X'pert Philip, Nickel-filtered Cu Kα radiation, 40 kV and 30 mA). The atomic force microscope (AFM) images were obtained using Nanoscope III AFM at room temperature. The cantilever used was micro-fabricated from Si_3N_4 and its spring constant was 0.03 Nm^{-1}. AFM imaging was operated by a tapping mode. The scanning direction was horizontal and towards the long axis of the cantilever. The X-ray photoelectron spectroscope (XPS) measurement was performed on a VG Scientific ESCALAB MK spectrometer with the Mg Kα X-ray source (1253.6 eV.). Samples in the form of casting film were mounted on a sample holder by double-sided adhesive tape. The X-ray source was run at a reduced power of 120 W. All core-level spectra were calibrated by the C 1s of neutral carbon peak, the binding energy (BE) of which is 284.6 eV. All spectra were obtained with a take-off angle of 75°C (with respect to the sample surface). The surface stoichiometry of elements was determined from peak-area ratios. After correcting with experimentally determined sensitivity factors, the values obtained are reliable, which have less than ±10% error. The surface morphology in a large scale was recorded using JSM-T330A SEM.

2.3. Water contact angle measurement

The static water contact angles were measured at 25°C and 60% relative humidity using a telescopic goniometer (Rame Hart Model 100-00(230)). The telescope with a magnification power of 23 × was equipped with a protractor of 1° graduation. For each angle reported, at least five sample readings were averaged. The angles reported are reliable to ±3°.

3. Results

3.1. Thermal analysis

The miscibility in a polymer blend arises from the interactions among amorphous segments of different components. For those components that are semi-crystallized, only the amorphous segments contribute to the miscibility of the blend. Hence, the T_m depression can be used to estimate the interaction parameter B between components in a binary blend [19]:

$$T_m^0 - T_m = -T_m^0 \frac{BV_{2u}}{\Delta H_{2u}} \phi_1^2 \quad (1)$$

In this equation, the subscript 1 and 2 represent the non-crystallizable and the crystallizable components, respectively. T_m^0 is the equilibrium melting points of component 2 in pristine state and T_m the corresponding temperature in the blend. ϕ_1 is the volume fraction of component 1 in the blend. $\Delta H_{2u}/V_{2u}$ is the latent heat of fusion per unit volume of component 2. For pristine PVDF, the $\Delta H_{2u}$and V_{2u} are 1600 cal mol^{-1} and 36.4 cm^3 mol^{-1}, respectively. When PVDF is blended with PVP, the melting point of it decreases with increasing the content of amorphous PVP (Fig. 1). A reduction of fusion heat (area of the peak) can also be observed in the sample with a high PVP content, for instance DFVP41. According to the above equation, B values of this blend are all negative as $T_m^0 - T_m > 0$, which is an indication of the existence of miscibility in the blend. When the content of PVP is further increased to 50 wt% (sample DFVP11), only one glass transition temperature rather than T_m can be detected, which means

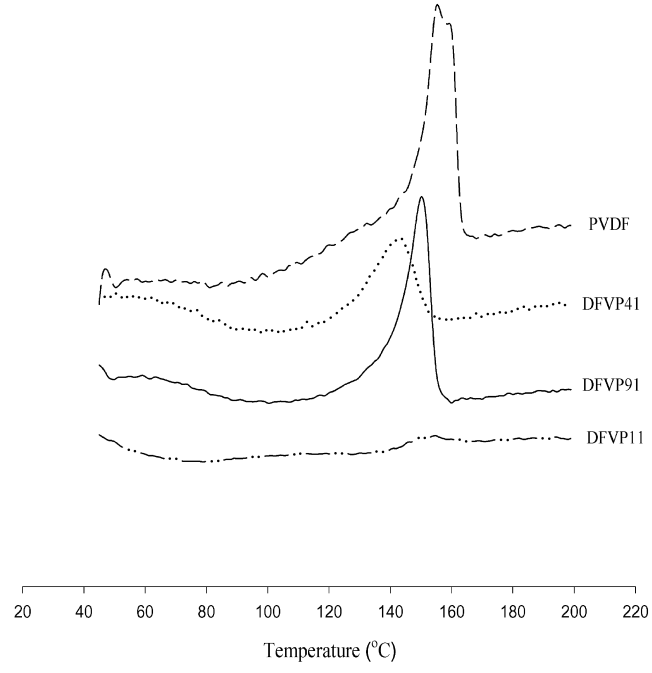

Fig. 1. DSC analysis of PVDF and the films consisting of PVDF and PVP by different proportions.

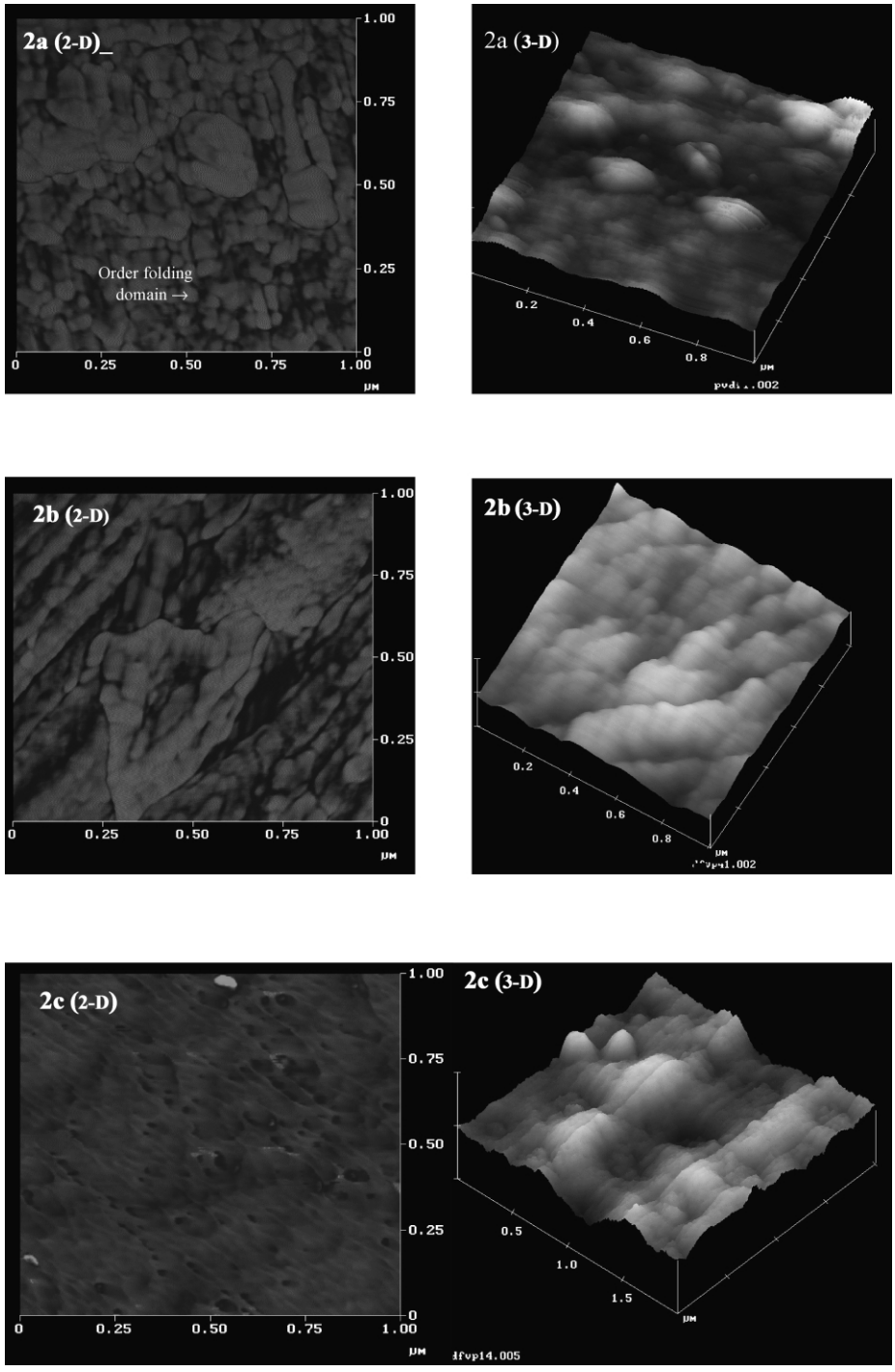

Fig. 2. AFM phase images of the casting films: (a) PVDF; (b) DFVP41; (c) DFVP14.

the crystalline phase of PVDF disappeared entirely in the bulk, and the blend became amorphous and miscible.

3.2. Atomic force microscope

The scanning range was limited in 1 μm, which is smaller than the dimension of a single crystal grain, so that local crystal structure can be detected. As the change in phase angle of the cantilever probe is sensed, the phase contrast image was obtained (Fig. 2 (2-D)). Although the phenomenon affecting phase image contrast is complex, the enhanced contrast that can be obtained often allows for distinguishing of different material phases [21]. The image of pristine PVDF film pinpoints the fine crystal structure on which one can see an array of light color domains. The light color domain seems to be generated from an order folding of PVDF segments, and the dark domain is likely due to the visco-elasticity response of the random entanglement of

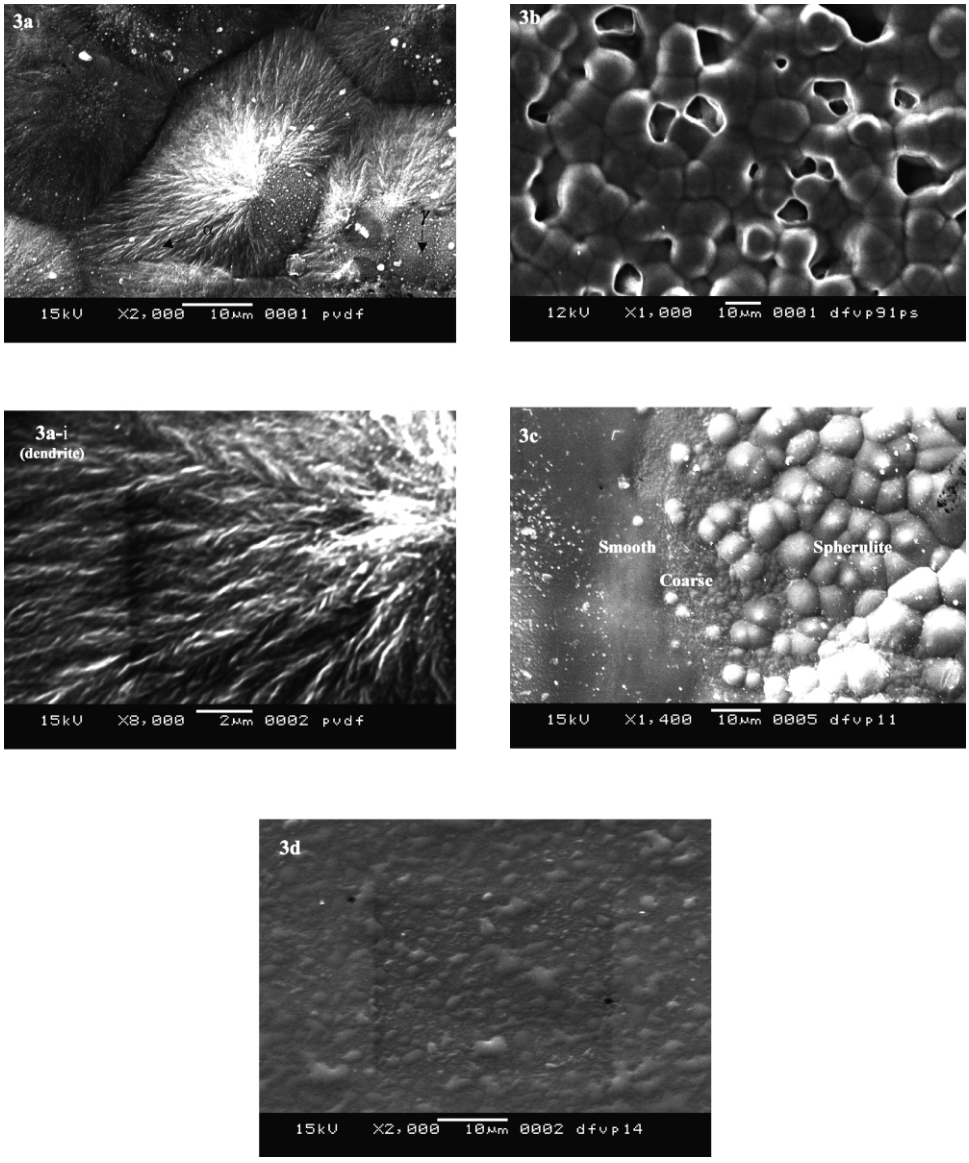

Fig. 3. SEM images of the casting films: (a) PVDF; (b) DFVP91; (c) DFVP11; (d) DFVP14.

segmental PVDF. After 20% PVP was blended in, the AFM image of the resulting DFPV41 film (Fig. 2(b) (2-D)) exhibited a similar topography except for the increased proportion of dark area. However, when the blend contains 80% PVP, the rather order array displayed by Fig. 2(a) and (b) of the microdomains is substituted by a continuous topography (Fig. 2(c) (2-D)), which serves as an indication of the thorough mixing between PVDF and amorphous PVP, with the PVDF no longer crystallizing in the film. To verify that the color distinction displayed in the 2-D image is not due to the variation in surface height gap but the true reflection of different material phases, the 3-D images have also been taken correspondingly (Fig. 2 (3-D)). It is clear that 2-D and 3-D do not share an identical pattern. For instance, although the height image of DFPV14 (Fig. 2(c) (3-D)) shows the hill–valley topography, its 2-D phase image exhibits no color distinction following its height image.

3.3. Scanning electron microscope

The topography of the films in a larger scale was pictured by SEM (Fig. 3). For pure PVDF, the surface is dominated by the typical dendrite crystalline phase and also contains a handful of spherulite phase (Fig. 3(a)); they have been described as the characteristics of α and γ phases, respectively [20]. The presence of PVP leads to changes in the surface topography (Fig. 3(b)–(d)). When the blend contains 10% PVP (sample DFVP91), the surface changes to the spherulite phase from the dendrite phase (Fig. 3(b)). Again, when the content of PVP is increased to 50% (sample DFVP11), the surface consists of both the spherulite phase domain and the plain domain (Fig. 3(c)). Further increasing PVP content to 80 wt% results in a surface without the characteristic morphology (Fig. 3(d)).

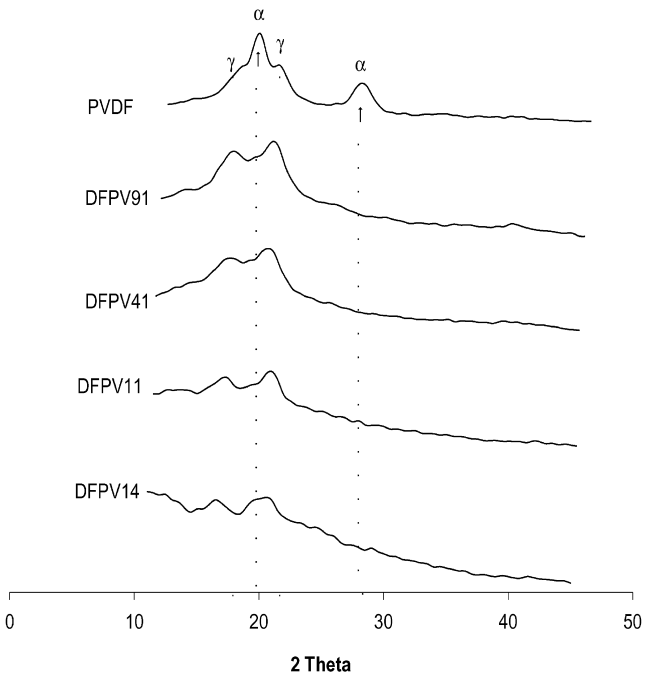

Fig. 4. XRD patterns of the surface phase of DFVP films.

3.4. X-ray diffractometry

The X'pert XRD system can provide two modes of beams with different incidental angles: upper beam and lower beam. The upper beam with a bigger incidental angle is used to identify structures of the bulk phase. The lower beam with a smaller incidental angle is used to detect the crystal structures near surface. The lower beam mode employed in this study (Fig. 4) shows that PVDF film gives a diffraction pattern consisting of four peaks. On the contrary, two of the peaks ($2\theta = 20$ and 28.5°) in the above pattern disappeared when 10% by weight of PVP was dispersed into PVDF. Correspondingly, the change in morphology from Fig. 3(a) to (b) supports the attribution of these two peaks to dendrite α phase. The remaining two peaks can be, therefore, regarded as the contribution of spherulite γ phase, as γ phase occurs also in PVDF (Fig. 3(a)). In Fig. 3(b), the surface of DFPV91 film possesses the grain-boundary structure. The XRD of this sample exhibits a pattern very similar to that of γ phase. It is thus believed that the grains are composed mainly of spherulite γ phase. With an increase in the PVP content in the blend, the peaks accredited to grain-boundary structure become weaker and appear at the smaller 2-theta values in contrast to those of spherulite γ phase. For DFVP14, its XRD pattern exhibits very weak diffraction peaks, indicating an amorphously predominated matrix exists in surface layer of the sample. This result is in agreement with the withdrawal of the grain-boundary structure from Fig. 3(d).

Table 1
Relative content of the two polymers on the surface of the films determined by XPS analysis

Casting films	Atomic ratio *F*/*N* (XPS)	Atomic ratio *F*/*N* (Feeding stock)	$(F/N)_{XPS}/(F/N)_{FS}$
DFVP91	15.90	31.2	0.5
DFVP41	12.43	13.88	0.9
DFVP11	7.10	3.47	2.1
DFVP14	2.33	0.87	2.7

3.5. X-ray photoelectron spectroscopy

XPS was employed to study the surface composition of the blend via determining the atomic ratio [*F*]/[*N*] since the detection depth by XPS is less than 10 nm. The surface compositions of different casting films are given in Table 1. The values of atomic ratio [*F*]/[*N*] of DFVP91 and DFVP41 are lower than those in the feeding stock. The general rule that surface prefers species with lower interfacial free energy are not applicable to these two films. However, the surface enrichment effect resumed in the cases of DFVP11 and DFVP14.

3.6. Contact angle measurement

The contact angle measurement shows that the surface hydrophobicity changes slightly when the content of PVDF decreases from 90 to 50%; the contact angle of water on the surface of DFVP11 is 72°, which is not overly distant from the 88° of pure PVDF. However, when the content of PVDF decreases further to 25% the contact angle decreases to 44°, which is a typical hydrophilic surface (Fig. 5). It is worth noting that despite the SEM image of a rather rough surface (e.g. Fig. 3(c)), the water-droplet used to conduct the contact angle measurement covers a sufficiently large area to give a reliable average value that is affected negligibly by the local roughness.

4. Discussions

4.1. Phase transition of PVDF in the DFVP blend

The chain conformation of PVDF building up the α phase is *trans–gauche* [20], placing the hydrogen and fluorine atoms alternately on each side of the chain. There is no steric strain between the *gem*-fluorine atoms and only minimal strain caused by adjacent hydrogen–fluorine interaction. However, once some segments of such a PVDF chain interact with segments of a PVP chain, the other segments of the PVDF chain will no longer keep the pure *trans–gauche* form that results in the dendrite α phase (Fig. 3(a)-i). The effect of interaction is very sensitive as long as a low content of PVP is present in the blend. Take for example the film of DFVP91 that contains 10% of PVP, whose surface has already been overwhelmed by spherulite γ phase (Fig. 3(b)). This explanation is also supported by the

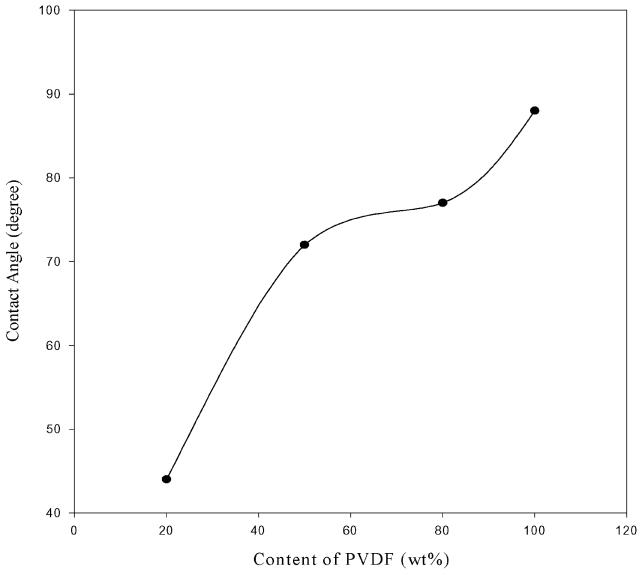

Fig. 5. The water contact angle measurement on different DFPV films.

XRD pattern (Fig. 4), on which the peaks characterizing α phase disappear.

In contrast to the DSC result, those obtained from AFM, XRD, XPS and SEM reflect specifically the information of the surface phase image, crystal structure, composition and morphology. Although the crystalline PVDF phases disappear with an increase in the content of PVP, the crystallization of PVDF at the surface is relatively less affected by PVP. A typical example is DFVP11, whose DSC diagram (Fig. 1) does not display any melting peak while the spherulite γ phase still exists at the surface according to its SEM image (Fig. 3(c)). It is rational that PVDF segments staying at the surface are subjected to less perturbation by the neighboring PVP segments than those located in the bulk phase.

4.2. FT-IR evidence of the intermonomeric hydrogen bonding

With respect to the nature of the interaction between PVDF and PVP, it is assumed that the quasi-hydrogen bonding occurs due to the fact that the hydrogen atoms of PVDF possess acidity and the oxygen atoms of PVP offer electronegativity. A comparison of FT-IR spectra of the pristine PVDF, PVP with the three DFVP samples clearly shows the occurrence of the hydrogen bonding (Fig. 6). The carbonyl stretching absorption band of PVP locating at 1667 cm^{-1} shifts to higher frequencies by up to 13 cm^{-1} with the increase in the content of PVP. This observation can be interpreted by the effect of forming hydrogen bond between the carbonyl group and the methylene group (Scheme 1); the hydrogen bonding restricts the vibration of C=O bond and hence increases the absorption frequency.

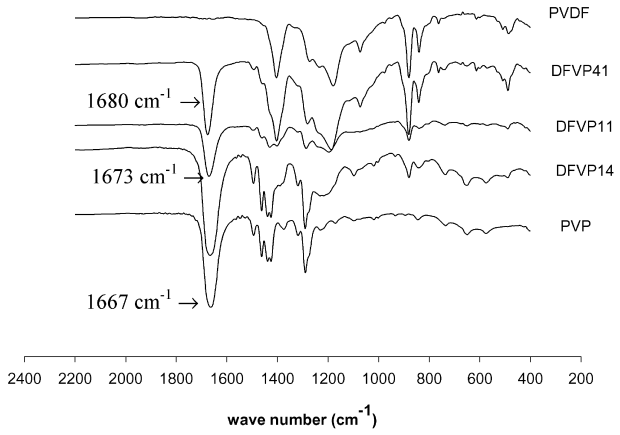

Fig. 6. FT-IR spectra of the DFPV films.

4.3. Formation of a sub-stable surface composition

Pursuant to Section 3.5, it is believed that the non-equilibrium surface state on DFVP91 and DFVP41 (Table 1) was developed during the drying process followed by the casting. According to XPS analysis, the *F*/*N* value of these two films is less at the surface than in the bulk. This fact suggests that excess PVP segments would have been brought to surface via, presumably, the attractive interaction between PVP and PVDF. It can be envisaged PVP segments have a greater extent to gain access to PVDF when its dosage in the feedstock is lower. Therefore, a higher percentage of PVP segments should be retained at the surface when its content is lower in the blend during drying. This effect is obvious when one inspects the surface enrichment scope of PVP on the DFVP91 and DFVP41 films (Table 1).

As far as the distribution of PVP segments at the surface of the VFPV91 film is concerned, PVP segments would most likely accumulate at boundaries of the crystalline PVDF grains, which are also exposed to the atmosphere (Scheme 2). Furthermore, amorphous PVDF/PVP stripes formed along the boundaries would perturb the crystallization of PVDF inside the grains. The perturbation then caused disbanding of the grains with the farther involvement of PVP segments as shown in the SEM image of sample DFVP11 (Fig. 3(c)), on which one can see contraction of the spherulite phase (in contrast to Fig. 3(b)). There is a coarse periphery between the spherulite phase and the smooth

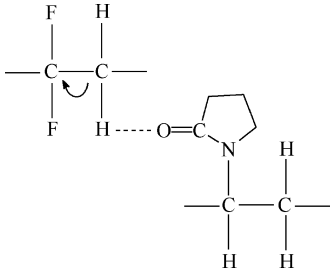

Scheme 1.

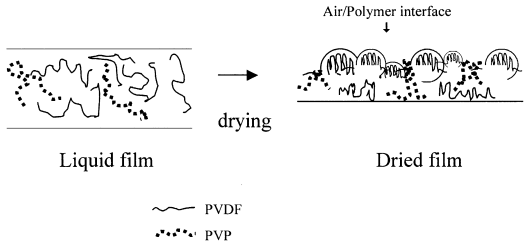

Scheme 2.

domain on DFVP11. As the uncharacteristic (smooth) morphology prevails in Fig. 4(c), (known to be the indication of an amorphously predominated matrix according to the XRD result), the coarse domain consisting of dispersed small crystal grains is, therefore, regarded as an intermediary structure between the crystal and the amorphous phases. With reference to the aforementioned shift of XRD patterns of γ-like phase, one can infer that the amorphism of PVDF takes place with the engagement of PVDF and PVP segments along the periphery of spherulite PVDF phase, as depicted in Scheme 2.

To verify the existence of thermodynamically non-equilibrium state at the surface, an annealing treatment of DFVP91 and DFVP41 was conducted at 120°C. For sample DFVP91, 48-h of annealing has brought the surface close to the thermodynamically equilibrium state (Fig. 7). It was found that the surface [*F*]/[*N*] values of these two films were lifted to 36.7 and 19.0, respectively, from original 15.9 and 12.43. The annealing treatment indeed freed the non-equilibrium state, and the surface of the films was therefore enriched by PVDF. For the other two samples, DFPV11 and DFPV41, the annealing had very little influence on the surface composition because the surface might have already been at the equilibrium state due to the enrichment of PVDF segments on these two films (Table 1). The surface enrichment effect is boosted with the PVP content (column 3 of Table 1), which satisfies the natural tendency.

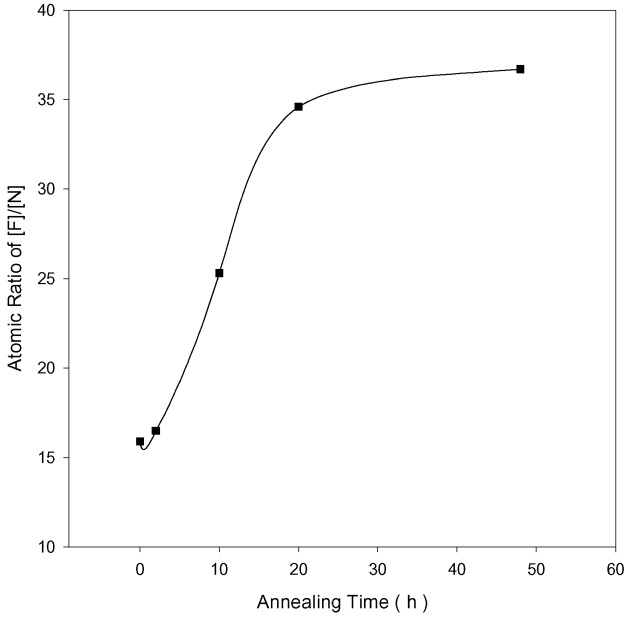

Fig. 7. Changes of the surface composition of DFVP91 film with the time span of annealing.

4.4. The factors that affect surface hydrophilicity

It can be seen that the curve of the water contact angle versus the composition of the film (Fig. 5) consists of three sections. The plateau section ranging from about 80 to 50% indicates the two transformation processes with an increase in PVP content: (1) the resume of surface enrichment tendency to PVDF; and (2) the contraction of the crystallization domains on the surface of film. The former process promotes the hydrophobicity while the later yields an opposite effect. Hence, a hydrophobic–hydrophilic equilibrium is approximately sustained across this plateau. In the section before the plateau, wherein the PVP content is greater, the surface of film consists chiefly of the amorphous PVDF/PVP matrix. Therefore, the PVP content at surface outweighs the hydrophilicity despite the fact that surface enrichment of PVDF is more severe in this stage than the others. In the section after the plateau, wherein the PVDF content is greater, the surface of film consists primarily of the crystalline PVDF grains and PVP besieging the PVDF phase. In this case, the loss of the hydrophobicity becomes apparent with the participation of PVP into the hydrophobically predominated surface.

5. Conclusions

PVDF possesses a strong tendency to undergo crystallization and to interact with amorphous PVP via the quasi-hydrogen bonding. The surface morphology and composition of the film comprising of these two homopolymers undergoes a series of changes with the content of PVP. When the PVP content is low (e.g. 10%), the interaction between the two polymers causes the conversion of polymorph from the highly steric demanded dendrite α phase to the grain-boundary structure, which is composed primarily of spherulite phase. When the PVP content is higher than 20%, the surface hydrophilicity rises slightly until the content of PVP reaches 50%. The surface enrichment of PVDF and the persistence of crystallized phase at the surface relative to that in the bulk offset the increment of the PVP content at surface. When the PVP content is greater than 50%, a visible increase in the surface hydrophilicity with the PVP content is displayed because there are no crystalline PVDF domains on the film. As a whole, the interaction between PVP and PVDF gives rise to surfacing of PVP, which subjects to an amphiphilic surface of the film.

References

[1] Paul DR, Barlow JW. J Macromol Sci, Rev (c) 1980;18:109.
[2] Magonov SN, Whangbo MH. Surface analysis with STM and AFM. Weinheim: VCH, 1996. Chapter 13.
[3] Duan YZ, Pearce EM. Polym Prepr 2000;41(1):971–2.
[4] Walia PS, Lawton JW, Shogren RL, Felker FC. Polymer 2000;41(22):8083–93.
[5] Yuan YM, Schoichet MS. Macromolecules 2000;33(13):4926–31.
[6] Oslanec R, Genzer J, Faldi A, Composto RJ, Garrett PD. Macromolecules 1999;32(12):4098–105.
[7] Zhao X, Zhao W, Skolov J, Rafailovich MH, Schwarz SA, Wilkens BJ, Jones RAL, Kramer EJ. Macromolecules 1991;24(22):5991–6.
[8] Pan DHK, Prest Jr WM. J Appl Phys 1985;58(8):2861–70.
[9] Schmidt JJ, Gardella JA, Salvati L. Macromolecules 1989;22(12):4489–95.
[10] Ermi BD, Karim A, Douglas JF. J Polym Sci, Part B: Polym Phys 1998;36(1):191–200.
[11] Thomas HR, O'Malley JJ. Macromolecules 1981;14(5):1316–20.
[12] Jamil T, Jamieson AM. J Polym Sci, Part B: Polym Phys 1989;27(12):2553–60.
[13] Hanhn BR, Hermann-Schonherr O, Wendorff JH. Polymer 1987;28:201–8.
[14] Kallitsis JK, Kalfoglou NK. Angew Makromol Chem 1987;148:103–17.
[15] Kammer HW, Kressler J, Kummerloewe C. Adv Polym Sci 1993;106:31–85.
[16] Yang H, Han CD, Kim JK. Polymer 1994;35(7):1503–11.
[17] Galin M. Makromol Chem 1987;188:1391.
[18] Ceccorulli G, Pizzoli M, Scandola M, Alfonso GC, Turturro A. Polymer 1989;30(7):1251–6.
[19] Lee WK, Ha CS. Polymer 1998;39(26):7131–4.
[20] Dohany JE, Humphrey JS. Vinylidene fluoride polymers. In: Kroschwitz JC, Mark HF, Bikales NM, Overberger CG, Menges G, editors. 2nd ed. Encyclopedia of polymer science and engineering, vol. 17. New York: Wiley, 1990. p. 537–48.
[21] Raghavan D, Gu X, Nguyen, VanLandingham M, Karim A. Macromolecules 2000;33:2573–83.